Resident Neural Stem Cells Restrict Tissue Damage and Neuronal Loss After Spinal Cord Injury in Mice

Hanna Sabelström *et al.*

Science **342**, 637 (2013);
DOI: 10.1126/science.1242576

Science (print ISSN 0036-8075; online ISSN 1095-9203) is published weekly, except the last week in December, by the American Association for the Advancement of Science, 1200 New York Avenue NW, Washington, DC 20005.

5. J. K. Baillie *et al.*, *Nature* **479**, 534–537 (2011).
6. G. D. Evrony *et al.*, *Cell* **151**, 483–496 (2012).
7. E. M. Ostertag, H. H. Kazazian, *Nature* **435**, 890–891 (2005).
8. T. Singer, M. J. McConnell, M. C. Marchetto, N. G. Coufal, F. H. Gage, *Trends Neurosci.* **33**, 345–354 (2010).
9. S. L. Martin, *Nature* **460**, 1087–1088 (2009).
10. D. M. Bushman, J. Chun, *Semin. Cell Dev. Biol.* **24**, 357–369 (2013).
11. E. Vanneste *et al.*, *Nat. Med.* **15**, 577–583 (2009).
12. N. Navin *et al.*, *Nature* **472**, 90–94 (2011).
13. K. L. Spalding, R. D. Bhardwaj, B. A. Buchholz, H. Druid, J. Frisén, *Cell* **122**, 133–143 (2005).
14. F. B. Dean *et al.*, *Proc. Natl. Acad. Sci. U.S.A.* **99**, 5261–5266 (2002).
15. A. Adey *et al.*, *Genome Biol.* **11**, R119 (2010).
16. R. S. Lasken, *Biochem. Soc. Trans.* **37**, 450–453 (2009).
17. R. S. Lasken, T. B. Stockwell, *BMC Biotechnol.* **7**, 19 (2007).
18. A. B. Olshen, E. S. Venkatraman, R. Lucito, M. Wigler, *Biostatistics* **5**, 557–572 (2004).
19. K. J. Brennand *et al.*, *Nature* **473**, 221–225 (2011).
20. L. C. Laurent *et al.*, *Cell Stem Cell* **8**, 106–118 (2011).
21. T. Baslan *et al.*, *Nat. Protoc.* **7**, 1024–1041 (2012).
22. A. Abyzov *et al.*, *Nature* **492**, 438–442 (2012).
23. C. E. Bruder *et al.*, *Am. J. Hum. Genet.* **82**, 763–771 (2008).
24. M. O'Huallachain, K. J. Karczewski, S. M. Weissman, A. E. Urban, M. P. Snyder, *Proc. Natl. Acad. Sci. U.S.A.* **109**, 18018–18023 (2012).
25. A. Piotrowski *et al.*, *Hum. Mutat.* **29**, 1118–1124 (2008).
26. E. Suberbielle *et al.*, *Nat. Neurosci.* **16**, 613–621 (2013).
27. T. Maeda *et al.*, *Biochem. Biophys. Res. Commun.* **319**, 1117–1123 (2004).
28. Y. Shibata *et al.*, *Science* **336**, 82–86 (2012).
29. N. Gilbert, S. Lutz-Prigge, J. V. Moran, *Cell* **110**, 315–325 (2002).
30. P. A. Callinan *et al.*, *J. Mol. Biol.* **348**, 791–800 (2005).
31. N. Gilbert, S. Lutz, T. A. Morrish, J. V. Moran, *Mol. Cell. Biol.* **25**, 7780–7795 (2005).
32. D. E. Symer *et al.*, *Cell* **110**, 327–338 (2002).
33. N. G. Coufal *et al.*, *Nature* **460**, 1127–1131 (2009).

Acknowledgments: We thank D. Husband (Salk), L. Moore (Salk), S. Jackmaert (KU Leuven), R. Layer (University of Virginia) and R. Clark (University of Virginia) for technical assistance; A. Prorock and Y. Bao (UVA Sequencing Core) for DNA sequencing; and all members of the Gage laboratory for critical feedback on the project. We thank M. L. Gage for editorial comments. F.H.G. thanks the Center for Academic Research and Training in Anthropogeny (CARTA) for support and perspective. This work was supported by a Crick-Jacobs Junior Fellowship to M.J.M.; a University of Leuven (KU Leuven) SymBioSys grant (PFV/10/016) to J.R.V. and T.V.; a Mather's Family Foundation grant, a NIH TR01 (R01 MH095741), the J.P.B. Foundation, Annette Merle-Smith, and a Helmsley Foundation grant to F.H.G.; and an NIH New Innovator Award (DP20D006493-01) and Burroughs Wellcome Fund Career Award to I.M.H. Human tissue was obtained from the National Institute for Child Health and Human Development (NIH) Brain and Tissue Bank for Developmental Disorders at the University of Maryland, Baltimore, MD, contract HHSN275200900011C, ref. no. N01-HD-9-011. The hiPSC lines used in this study are available from the Coriell Cell Repository. Microarray data have been deposited in the National Center for Biotechnology Information (NCBI) Gene Expression Omnibus (GSE51538), and DNA sequence data have been deposited in the NCBI Short-Read Archive (SRP030642).

Supplementary Materials

www.sciencemag.org/content/342/6158/632/suppl/DC1
Materials and Methods
Figs. S1 to S11
Tables S1 to S3
References (*34*–*46*)

19 July 2013; accepted 1 October 2013
10.1126/science.1243472

Resident Neural Stem Cells Restrict Tissue Damage and Neuronal Loss After Spinal Cord Injury in Mice

Hanna Sabelström,[1] Moa Stenudd,[1] Pedro Réu,[1,2] David O. Dias,[1] Marta Elfineh,[1] Sofia Zdunek,[1] Peter Damberg,[3] Christian Göritz,[1] Jonas Frisén[1]*

Central nervous system injuries are accompanied by scar formation. It has been difficult to delineate the precise role of the scar, as it is made by several different cell types, which may limit the damage but also inhibit axonal regrowth. We show that scarring by neural stem cell–derived astrocytes is required to restrict secondary enlargement of the lesion and further axonal loss after spinal cord injury. Moreover, neural stem cell progeny exerts a neurotrophic effect required for survival of neurons adjacent to the lesion. One distinct component of the glial scar, deriving from resident neural stem cells, is required for maintaining the integrity of the injured spinal cord.

Scar formation in the injured spinal cord limits secondary damage by providing mechanical stability and restricting infiltration by inflammatory cells (*1*–*3*) but also contributes to the failure of severed axons to regrow (*2*, *4*–*6*). Resident neural stem cells give rise to the majority of new astrocytes making the glial scar in the injured spinal cord (*7*, *8*). Transplantation of stem cells, or stem cell–derived cells, to the injured spinal cord can improve functional recovery (*9*). The mechanisms underlying this effect are not fully understood, but trophic effects as well as remyelination of spared axons appear most important (*9*–*13*). Modulating the response of endogenous neural stem cells may offer an alternative to cell transplantation, but this requires an understanding of the function of these cells in response to spinal cord injury.

[1]Department of Cell and Molecular Biology, Karolinska Institute, SE-171 77 Stockholm, Sweden. [2]Center for Neuroscience and Cell Biology, University of Coimbra, 3004-517 Coimbra, Portugal. [3]Department of Clinical Science, Intervention and Technology, Karolinska Institute, SE-171 77 Stockholm, Sweden.

*Corresponding author. E-mail: jonas.frisen@ki.se

The neural stem cells in the adult mouse spinal cord constitute a small cell population, denoted ependymal cells, lining the central canal (*8*, *14*–*16*). To address the role of ependymal cells in the spinal cord injury response, we selectively blocked their generation of progeny by deleting all *Ras* genes, which are required for cells to go through the G_1 phase of mitosis (*17*, *18*). We established FoxJ1-CreER mice, which allow conditional genetic recombination specifically in ependymal cells in the adult spinal cord after administration of tamoxifen (*8*), homozygous for *H-Ras* and *N-Ras* null alleles and homozygous for floxed *K-Ras* alleles (*17*). The mice also carried a *R26R-YFP* (YFP, yellow fluorescent protein) reporter allele to allow visualization of recombination. Tamoxifen was administered to adult mice to delete *K-Ras* (we refer to these mice as FoxJ1-rasless), and matched mice with the same genotype receiving vehicle (referred to as FoxJ1 mice) were used as controls (fig. S1).

Ependymal cell proliferation was selectively reduced in the intact spinal cord (Fig. 1, A and B), as well as after a dorsal funiculus incision in FoxJ1-rasless mice (Fig. 1, C to E, and fig. S2, A to E). Ependymal cell progeny starts migrating from the ependymal layer toward the injury site within 3 days after injury in control mice, where it almost exclusively differentiates to scar-forming astrocytes (*7*, *8*, *14*, *19*). There was no migration of recombined cells from the ependymal layer in FoxJ1-rasless mice (Fig. 1F and fig. S2, F and G), establishing this as a suitable system for assessing the role of neural stem cell progeny after spinal cord injury.

We made transverse incisions by cutting the dorsal funiculus and dorsal horns at C4 in matched FoxJ1 and FoxJ1-rasless mice (n = 14 in each group), and we analyzed these animals 14 weeks later. All FoxJ1 control mice developed a dense glial scar at the site of the lesion (Fig. 1G). In contrast, only 3 out of 14 FoxJ1-rasless mice developed largely normal scars at the injury site. The majority of FoxJ1-rasless mice (79%) failed to form compact scar tissue and had varying degrees of tissue defects, ranging from small cavities (21%) and less compact scars with larger cavities (29%) to a single large cyst (29%) occupying the lesion area (Fig. 1, H to J).

Pericytes play a key role in spinal cord scar formation by giving rise to the fibrotic compartment of the scar (*18*). The fibrotic compartment was enlarged in FoxJ1-rasless mice compared with FoxJ1 control mice, suggesting that increased fibrosis may partly compensate for the absence of ependymal cell progeny (fig. S3A). Similarly, there appeared to be a compensatory increase in scarring by resident astrocytes, which were unrecombined and not deriving from ependymal cells (Fig. 1, G to J, and fig. S3B). Resident astrocytes are molecularly and, potentially, functionally distinct from astrocytes generated by ependymal cells, which are mostly negative for glial fibrillary acidic protein (*8*). In addition to resident astrocytes (*20*), oligodendrocyte lineage cells have also been suggested to generate scar-forming astrocytes in the

injured forebrain (*21*), but this is not the case in the spinal cord (*7*, *16*).

After the 14-week recovery period, remaining lesions in FoxJ1-rasless mice were considerably deeper, the area of damaged tissue was larger, and the spinal cord at the site of the lesion was thinner compared with FoxJ1 control animals (Fig. 2, A to C, and fig. S3, C and D). In contrast, mice with blocked pericyte response, which fail to seal the lesion and regain tissue integrity (*18*), did not have lesions extending deeper or increased atrophy compared with control animals (fig. S4).

To assess the consequence of enlarged lesions, we examined the integrity of the corticospinal tract, a major axonal tract located immediately ventral to the lesion in this paradigm. Scar tissue penetrated the corticospinal tract in 1 of 14 FoxJ1 control mice (Fig. 2D). In contrast, the scar tissue and tissue defects extended through and disrupted the corticospinal tract in 9 of 14 FoxJ1-rasless mice (Fig. 2, E and F) ($P = 0.002$, Fisher's exact test), suggesting that secondary enlargement of the lesion in the absence of scarring by ependymal cell progeny severed the corticospinal tract and, potentially, other axons.

To delineate the time course for the extension of the lesions in FoxJ1-rasless mice, we followed additional cohorts of FoxJ1-rasless ($n = 6$) and FoxJ1 control animals ($n = 10$) longitudinally by magnetic resonance imaging (MRI). The first scan was made within 2 hours after injury, to establish the depth of the original lesion (524 ± 102 μm in FoxJ1-rasless and 584 ± 63 μm in FoxJ1 control mice, mean ± SEM, $P = 0.60$). Lesions in FoxJ1 control animals gradually contracted with 17% of their initial depth at 9 weeks after injury. Lesion depth was reduced in 6 of 10 FoxJ1 mice and unaltered (±5% compared to initial lesion) in the remaining mice after 9 weeks. In contrast, there was a gradual extension of lesions by 29% at 9 weeks in FoxJ1-rasless mice. Lesion depth was extended in all FoxJ1-rasless mice (Fig. 2, G and H). The difference in the change in depth with time between FoxJ1 and FoxJ1-rasless animals was first statistically significant at the 3-week time point ($P = 0.003$ for week 3, Student's t test; $P = 0.002$ for all time points, analysis of covariance). Three-dimensional (3D) reconstruction of magnetic resonance images revealed that the lateral extension of the lesion was reduced over time in both FoxJ1 and FoxJ1-rasless animals, whereas lesions extended centrally to become deeper in only FoxJ1-rasless animals (Fig. 2, G to I, and movies S1 to S4).

The glial scar is normally compartmentalized with resident astrocytes forming the periphery of the scar and ependymal cell–derived astrocytes forming the central part (*7*). Reactive astrocytes are implicated in restricting the infiltration of inflammatory cells and protecting against the secondary damage they cause (*2*, *3*). However, the secondary damage in FoxJ1-rasless mice was not preceded by increased infiltration of inflammatory cells. In contrast, fewer inflammatory cells were present in the injured spinal cord segment of FoxJ1-rasless mice compared with FoxJ1 mice ($P = 0.03$) (fig. S5). This finding suggests that restricting the secondary damage caused by inflammation may be a specific function for resident astrocytes, whereas ependymal cell–derived astrocytes may primarily be required to reinforce the injured spinal cord.

The atrophy of the spinal cord in FoxJ1-rasless mice extended two segments rostral and caudal to the lesion. More distant spinal cord segments were unaffected (Fig. 3A and fig. S6A). Analysis of the thickness of the spinal cord at the time of lesion and 9 weeks after injury in the same animals by MRI confirmed the increased atrophy in the absence of neural stem cell progeny (Fig. 3B). Quantification of the number of neurons revealed an ~20% increase in neuronal loss in FoxJ1-rasless mice compared with FoxJ1 control mice 14 weeks after injury (Fig. 3C), largely restricted to the dorsal horn (fig. S6B). Specific neuronal subpopulations in the dorsal horn were differentially affected: 64 to 66% of neurokinin-1 receptor–expressing projection neurons in lamina 1 and 32 to 46% of calbindin-expressing interneurons were lost, whereas the

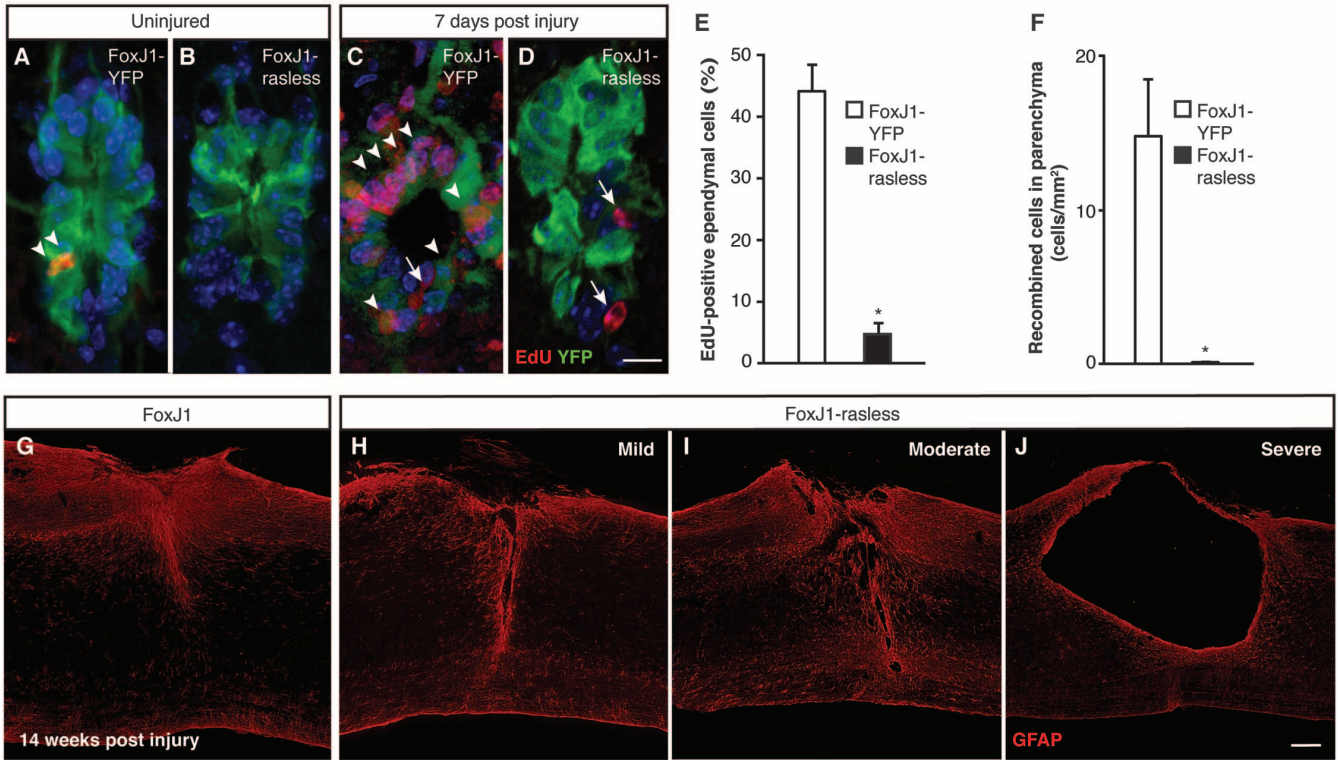

Fig. 1. Impaired scar formation in the absence of neural stem cell progeny. Ependymal cell incorporation of 5-ethynyl-2′-deoxyuridine is reduced in the absence of *Ras* genes in intact spinal cord (**A** and **B**) and 7 days after injury (**C** to **E**). Arrowheads and arrows point to proliferating recombined (A and C) and unrecombined (C and D) ependymal cells, respectively. Injury-induced migration is blocked in rasless ependymal cells (**F**). Sagittal view of the lesion site 14 weeks after injury in a FoxJ1 control mouse (**G**) and FoxJ1-rasless mice (**H** to **J**). Recombined ependymal cells express YFP in (A) to (D), and cell nuclei are labeled with 4′,6-diamidino-2-phenylindole (DAPI) and appear blue. *$P < 0.05$, **$P < 0.01$; Student's t test. Error bars show SEM. Scale bars represent 10 μm in (A) to (D) and 200 μm in (G) to (J). GFAP, glial fibrillary acidic protein.

number of protein kinase C γ (PKCγ)–positive interneurons in lamina 2 was unaffected in FoxJ1-rasless mice compared with FoxJ1 mice (Fig. 3, D to F). The degree of neuronal loss did not correlate to injury depth (coefficient of determination $r^2 = 0.013$ caudal and $r^2 = 0.016$ rostral to the injury), suggesting that it may not be a direct consequence of the enlarged lesions in FoxJ1-rasless mice. Furthermore, mice in which we had

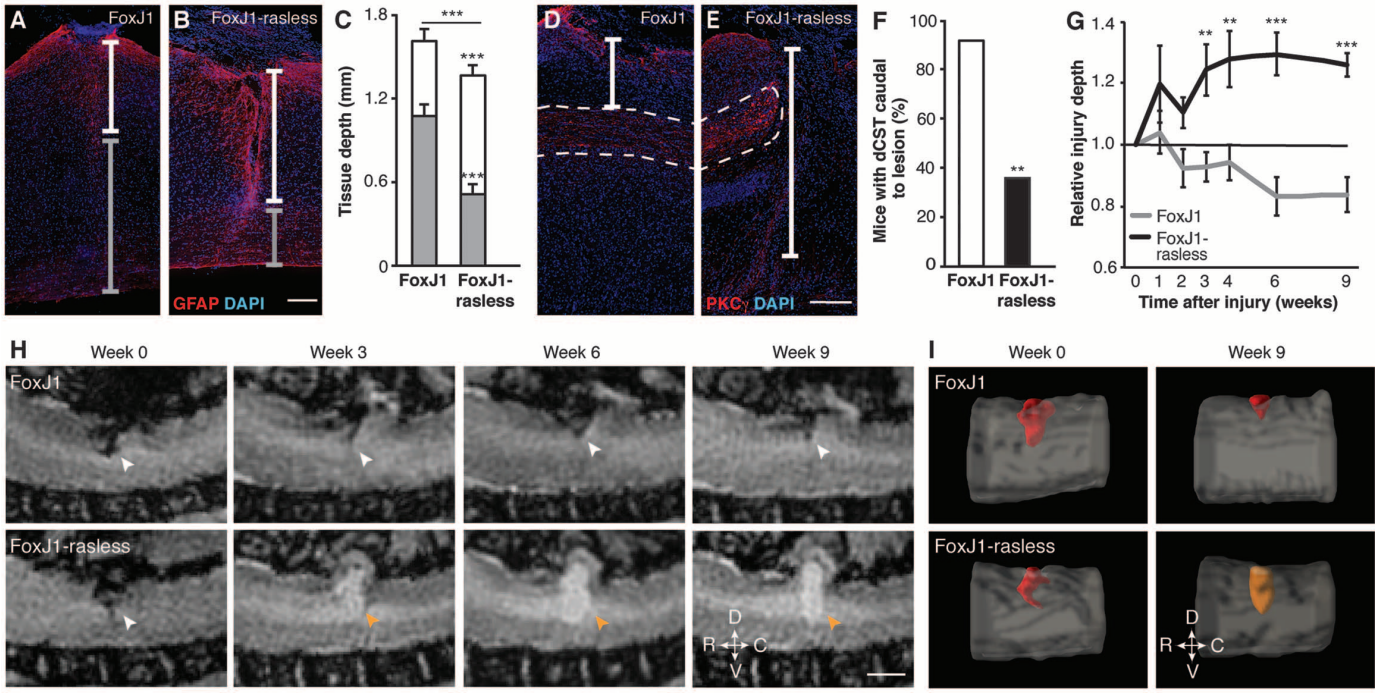

Fig. 2. Neural stem cell progeny reduces tissue damage after spinal cord injury. Glial scars (white markers) are deeper and less tissue is spared (gray markers) in the spinal cord 14 weeks after injury in FoxJ1-rasless mice (**A** to **C**). The dorsal corticospinal tract (dCST) marked by PKCγ (white dashed outline) is more frequently severed in FoxJ1-rasless mice compared with FoxJ1 control mice (**D** to **F**). Magnetic resonance images show increasing injury depth in FoxJ1-rasless mice and contraction of the lesion in FoxJ1 control mice (**G**). Serial magnetic resonance images of a lesion (white arrowheads) in a FoxJ1 control mouse and a lesion developing a cyst (orange arrowheads) in a FoxJ1-rasless mouse (**H**). 3D reconstruction of magnetic resonance images in (H) show reduced lesion size (red) in a FoxJ1 mouse and a cyst (orange) in a FoxJ1-rasless mouse (**I**). D, dorsal; V, ventral; R, rostral; C, caudal. $^{**}P < 0.01$, $^{***}P < 0.001$; Student's *t* test (C and G), Fisher's exact test (F). Error bars show SEM. Scale bars represent 200 μm in (A), (B), (D), and (E) and 1 mm in (H).

Fig. 3. Neuronal loss in the absence of neural stem cell–derived scar tissue. Increased spinal cord atrophy in segments adjacent to the lesion in FoxJ1-rasless mice 14 weeks after injury (**A**). Spinal cord thickness measured in magnetic resonance images 0 and 9 weeks after injury shows an increased atrophy in FoxJ1-rasless mice (**B**). The total number of neurons is reduced in segments adjacent to the lesion of FoxJ1-rasless mice 14 weeks after injury (**C**). NK1R-positive projection neurons (**D**) and calbindin-positive interneurons (**E**) are preferentially lost, whereas there is no reduction in the number of PKCγ-positive interneurons (**F**). seg, segments. $^{*}P < 0.05$, $^{**}P < 0.01$, $^{***}P < 0.001$; Student's *t* test. ns, not significant. Error bars show SEM.

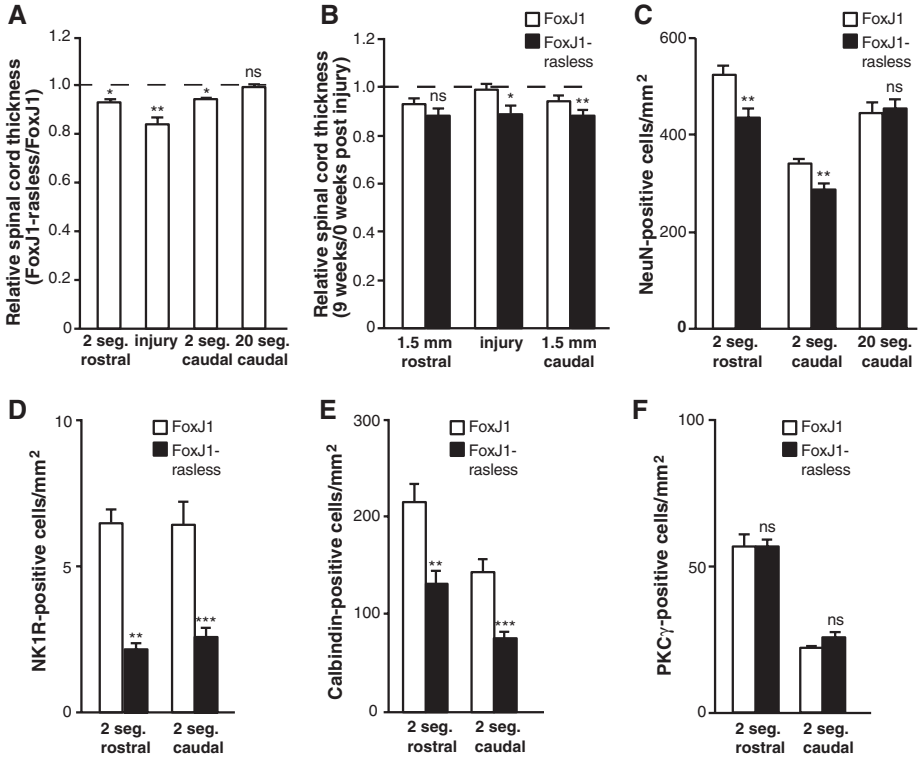

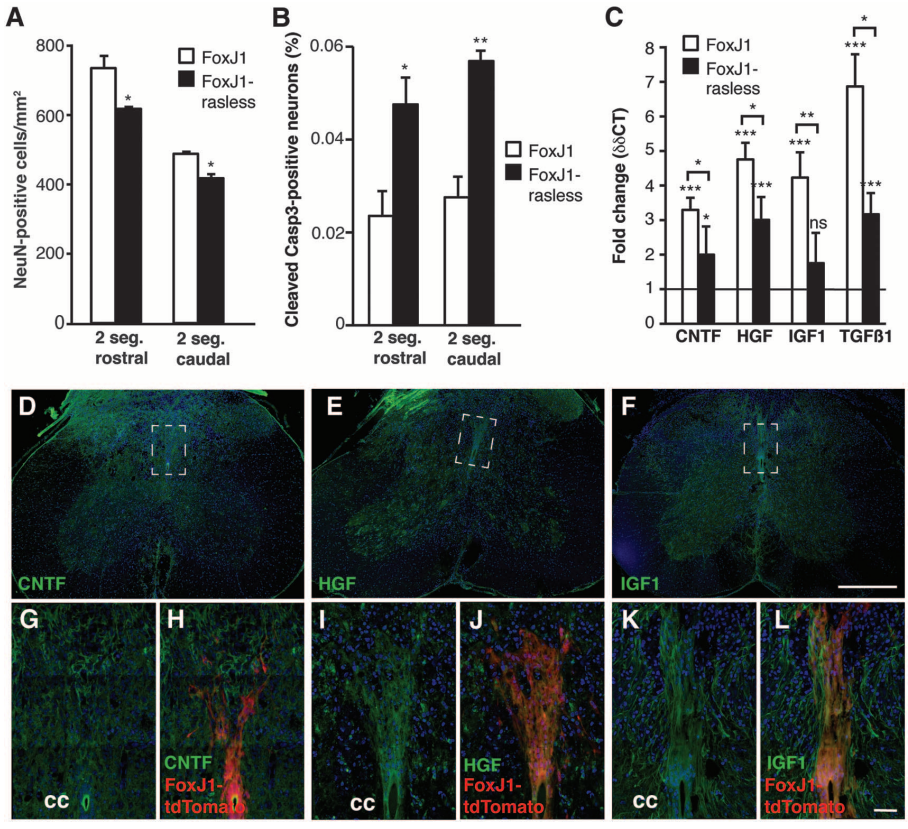

Fig. 4. Neural stem cell progeny is a major source of neurotrophic support after spinal cord injury. The number of neurons in segments adjacent to the lesion (**A**) and neurons undergoing apoptosis (**B**) 14 days after injury. mRNA levels of neurotrophic factors 14 days after injury compared with uninjured control mice (horizontal line) (**C**). FoxJ1-rasless mice have a reduced expression of neurotrophic factors 14 days after injury compared with FoxJ1 control mice (C). δδCT, delta delta cycle threshold. Ependymal progeny (red) expresses CNTF, HGF, and IGF-1 (**D** to **L**) 14 days after injury in control mice. Boxed areas in (D) to (F) are showed in higher magnification in (G) to (L). cc, central canal. *$P < 0.05$, **$P < 0.01$, ***$P < 0.001$;, Student's *t* test. Error bars show SD. Scale bars represent 500 μm in (D) to (F) and 50 μm in (G) to (L).

blocked scarring by pericyte-derived cells did not have increased neuronal loss or atrophy (fig. S6, C and D). Together, these findings suggest that the neuronal loss in FoxJ1-rasless mice may be independent from the deficient scarring and secondarily extended lesions and that ependymal cell progeny may have a trophic effect on nearby neurons.

We analyzed the number of neurons in FoxJ1 and FoxJ1-rasless mice at an earlier time point in an additional cohort of animals ($n = 3$ in each group). Approximately half the number of neurons that were lost at 14 weeks had already been lost 2 weeks after injury; neuronal death continued in subsequent weeks (Fig. 4A). Quantification of the number of cleaved caspase 3–positive apoptotic neurons demonstrated an increased number of dying neurons in the absence of ependymal cell progeny 2 weeks after injury (Fig. 4B), establishing this as a relevant time point to assess potential mechanisms for the increased neuronal loss in the absence of neural stem cell progeny.

Brain and spinal cord lesions trigger the production of neurotrophic factors (*22*, *23*), although the importance of this has been unknown. We confirmed the previously reported increased expression of *CNTF*, *HGF*, *IGF-1*, and *TGFß1* (CNTF, ciliary neurotrophic factor; HGF, hepatocyte growth factor; IGF, insulin-like growth factor; TGFβ, transforming growth factor–β) mRNA in the injured spinal cord (*22*, *24*, *25*) (Fig. 4C). Experimental administration of some of the corresponding proteins promotes neuronal survival after spinal cord injury (*13*, *24*, *26*), indicating that the endogenous levels are limiting. Immunohistochemistry in the injured spinal cord of control mice demonstrated that CNTF, HGF, and IGF-1 were synthesized by ependymal cell–derived astrocytes (Fig. 4, D to L, and fig. S7). FoxJ1-rasless mice had a statistically significant 47 to 77% attenuation of the up-regulation of mRNA for the neurotrophic factors (Fig. 4C). This finding establishes neural stem cell–derived cells as a major source of neurotrophic support after spinal cord injury and may explain the increased neuronal loss in the absence of ependymal cell progeny in FoxJ1-rasless mice.

Reducing scar formation has been a goal in many therapeutic strategies, but given our results, inhibiting scar formation by endogenous neural stem cells in the injured spinal cord does not appear attractive. Transplantation of spinal cord neural stem cells, which mainly give rise to astrocytes, promotes functional recovery (*27*). Steering the differentiation of these cells so that they also give rise to substantial numbers of remyelinating oligodendrocytes further improves the outcome (*27*). Thus, rather than suppressing scarring by resident neural stem cells, it is interesting to consider augmenting or modulating this response after spinal cord injury.

References and Notes

1. M. Pekny *et al.*, *J. Cell Biol.* **145**, 503–514 (1999).
2. S. Okada *et al.*, *Nat. Med.* **12**, 829–834 (2006).
3. J. E. Herrmann *et al.*, *J. Neurosci.* **28**, 7231–7243 (2008).
4. J. W. Fawcett, *J. Neurotrauma* **23**, 371–383 (2006).
5. J. Silver, J. H. Miller, *Nat. Rev. Neurosci.* **5**, 146–156 (2004).
6. M. V. Sofroniew, *Trends Neurosci.* **32**, 638–647 (2009).
7. F. Barnabé-Heider *et al.*, *Cell Stem Cell* **7**, 470–482 (2010).
8. K. Meletis *et al.*, *PLOS Biol.* **6**, e182 (2008).
9. F. Barnabé-Heider, J. Frisén, *Cell Stem Cell* **3**, 16–24 (2008).
10. J. Yan, A. M. Welsh, S. H. Bora, E. Y. Snyder, V. E. Koliatsos, *J. Comp. Neurol.* **480**, 101–114 (2004).
11. P. Lu, L. L. Jones, E. Y. Snyder, M. H. Tuszynski, *Exp. Neurol.* **181**, 115–129 (2003).
12. A. Yasuda *et al.*, *Stem Cells* **29**, 1983–1994 (2011).
13. K.-S. Hung *et al.*, *J. Neurosurg. Spine* **6**, 35–46 (2007).
14. C. B. Johansson *et al.*, *Cell* **96**, 25–34 (1999).
15. C. V. Pfenninger, C. Steinhoff, F. Hertwig, U. A. Nuber, *Glia* **59**, 68–81 (2011).
16. H. Sabelström, M. Stenudd, J. Frisén, *Exp. Neurol.* 10.1016/j.expneurol.2013.01.026 (2013).
17. M. Drosten *et al.*, *EMBO J.* **29**, 1091–1104 (2010).
18. C. Göritz *et al.*, *Science* **333**, 238–242 (2011).
19. A. J. Mothe, C. H. Tator, *Neuroscience* **131**, 177–187 (2005).
20. A. Buffo *et al.*, *Proc. Natl. Acad. Sci. U.S.A.* **105**, 3581–3586 (2008).
21. J. Kohyama *et al.*, *Proc. Natl. Acad. Sci. U.S.A.* **105**, 18012–18017 (2008).
22. G. W. J. Hawryluk *et al.*, *Stem Cells Dev.* **21**, 2222–2238 (2012).
23. M. Nieto-Sampedro *et al.*, *Science* **217**, 860–861 (1982).
24. K. Kitamura *et al.*, *J. Neurosci. Res.* **85**, 2332–2342 (2007).
25. R. B. Tripathi, D. M. McTigue, *J. Comp. Neurol.* **510**, 129–144 (2008).
26. J. Ye *et al.*, *Brain Res.* **997**, 30–39 (2004).
27. C. P. Hofstetter *et al.*, *Nat. Neurosci.* **8**, 346–353 (2005).

Acknowledgments: We thank F. Barnabé-Heider and O. Bergmann for discussions and M. Barbacid for providing *Ras* mutant mice through a materials transfer agreement with Centro Nacional de Investigaciones Oncológicas (Spanish National Cancer Institute, CNIO), Spain. Requests for mice should be directed to M. Barbacid (CNIO, Spain). This study was supported by the Swedish Research Council, the Swedish Cancer Society, the Karolinska Institute, Tobias Stiftelsen, AFA Försäkringar, StratRegen, and Knut och Alice Wallenbergs Stiftelse. D.O.D. and P.R. were supported by the Foundation for Science and Technology from the Portuguese government (SFRH/BD/63164/2009 and SFRH/BD/33465/2008).

Supplementary Materials

www.sciencemag.org/content/342/6158/637/suppl/DC1
Supplementary Text
Figs. S1 to S7
Movies S1 to S4

28 June 2013; accepted 23 September 2013
10.1126/science.1242576